HHS Public Access

Author manuscript

*FASEB J.* Author manuscript; available in PMC 2023 January 01.

Published in final edited form as:

*FASEB J.* 2022 January ; 36(1): e22069. doi:10.1096/fj.202100600RRR.

# Guanylyl cyclase-A phosphorylation decreases cardiac hypertrophy and improves systolic function in male, but not female, mice

**Brandon M. Wagner**[a], **Jerid W. Robinson**[b], **Chastity L. Healy**[a], **Madeline Gauthier**[a], **Deborah M. Dickey**[b], **Siu-Pok Yee**[d], **John W. Osborn**[c], **Timothy D. O'Connell**[a,*], **Lincoln R. Potter**[a,b,*]

[a]Department of Integrative Biology and Physiology, University of Minnesota, Medical School, Minneapolis, MN 55455 USA,

[b]Department of Biochemistry, Molecular Biology, and Biophysics, University of Minnesota, Medical School, Minneapolis, MN 55455 USA,

[c]Department of Surgery at the University of Minnesota, Medical School, Minneapolis, MN 55455 USA,

[d]Department of Cell Biology at the University of Connecticut Health Center, Farmington, CT 06030 USA

## Abstract

Atrial natriuretic peptide (NP) and BNP increase cGMP, which reduces blood pressure and cardiac hypertrophy by activating guanylyl cyclase (GC)-A, also known as NPR-A or Npr1. Although GC-A is highly phosphorylated, and dephosphorylation inactivates the enzyme, the significance of GC-A phosphorylation to heart structure and function is unknown. To identify *in vivo* processes that are regulated by GC-A phosphorylation, we substituted glutamates for known phosphorylation sites to make GC-A$^{8E/8E}$ mice that express an enzyme that cannot be inactivated by dephosphorylation. GC-A activity, but not protein, was increased in heart and kidney membranes from GC-A$^{8E/8E}$ mice. Activities were 3-fold higher in female compared to male cardiac ventricles. Plasma cGMP and testosterone were elevated in male and female GC-A$^{8E/8E}$ mice, but aldosterone was only increased in mutant male mice. Plasma and urinary creatinine concentrations were decreased and increased, respectively, but blood pressure and heart rate were unchanged in male GC-A$^{8E/8E}$ mice. Heart weight to body weight ratios for GC-A$^{8E/8E}$ male, but not female, mice were 12% lower with a 14% reduction in cardiomyocyte cross sectional area. Subcutaneous injection of fsANP, a long-lived ANP analog, increased plasma cGMP and decreased aldosterone in male GC-A$^{WT/WT}$ and GC-A$^{8E/8E}$ mice at 15 minutes, but only GC-A$^{8E/8E}$ mice had elevated levels of plasma cGMP and aldosterone at 60 minutes.

*Corresponding authors: Timothy D O'Connell tdoconne@umn.edu, Lincoln R Potter potter@umn.edu.

AUTHOR CONTRIUTIONS

BMW, JWR and LRP were responsible for experimental design. CLH and TDO were responsible for echocardiography design, analysis and interpretation. MG and JWO were responsible for telemetry blood pressure measurements and interpretation. BMW, JWR and LRP were responsible for heart histology and analysis. BMW and JWR were responsible for hormone analysis. BMW was responsible for cGMP and ERK1/2 analysis. BMW and LRP were responsible interpretation of all data. BMW, JWR and LRP wrote the manuscript. All authors reviewed the manuscript before submission.

CONFLICT OF INTERST

The authors declare no conflict of interest.

fsANP reduced ventricular ERK1/2 phosphorylation to a greater extent and for a longer time in the male mutant compared to WT mice. Finally, ejection fractions were increased in male but not female hearts from GC-A$^{8E/8E}$ mice. We conclude that increased phosphorylation-dependent GC-A activity decreases cardiac ERK activity, which results in smaller male hearts with improved systolic function.

## Graphical Abstract

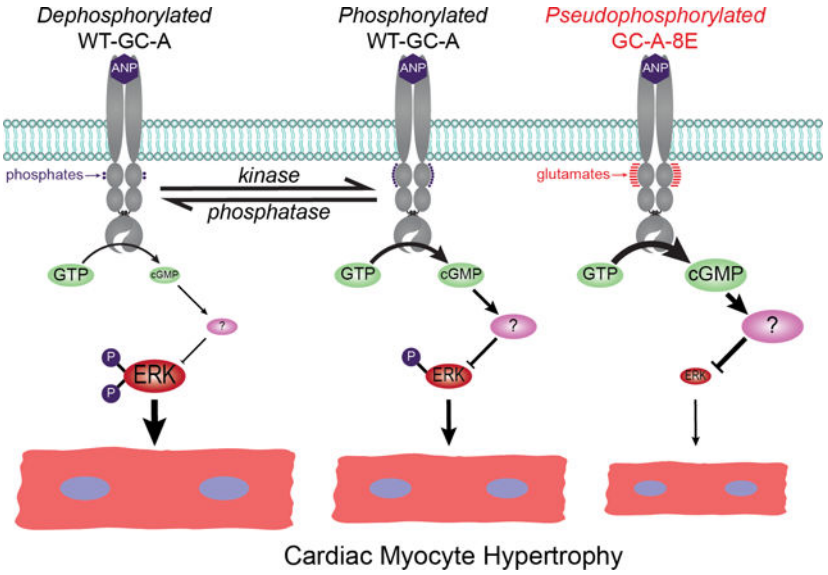


### Keywords

cardiac hypertrophy; natriuretic peptide; hypertension; guanylyl cyclase; extracellular regulated kinase

## 1. INTRODUCTION

In response to volume overload, atrial natriuretic peptide (ANP) and B-type NP (BNP) are released from the heart into the blood, where they decrease blood pressure by stimulating vasorelaxation, natriuresis, diuresis and endothelial permeability (1, 2). All of these responses are mediated through direct activation of guanylyl cyclase (GC)-A because GC-A knock out mice do not respond to cardiac NPs, are hypertensive, and display cardiac hypertrophy, whereas mice lacking the NP clearance receptor (NPR-C), the other receptor for ANP and BNP, display phenotypes associated with increased NP-stimulated GC activity (3–7). Although GC-A-dependent reductions in blood pressure were initially hypothesized to indirectly decrease cardiac hypertrophy (6), elegant pharmacologic and genetic studies demonstrated that GC-A reduces cardiac hypertrophy independently of blood pressure (8–11) by an unknown mechanism that occurs early in development (12).

Both GC-A and GC-B, a homologous receptor that is activated by C-type NP (13), are phosphorylated on multiple conserved serines and threonines under basal conditions (14–20). However, prolonged exposure to NPs or acute exposure to luteinizing hormone (21,

22) or fibroblast growth factor for GC-B (23, 24), or possibly angiotensin II for GC-A (11, 25, 26), cause the dephosphorylation and inactivation of these receptors. Multiple homologous phosphorylation sites were first identified in GC-A and GC-B (14, 15, 17–20, 27–29), but were later identified in the retinal GC known as GC-1 or GC-E (30) and a receptor GC expressed in sea urchin sperm (31). Alanine substitutions that mimic uncharged, dephosphorylated residues, result in reduced NP-dependent GC activities (18, 19, 28), and the mutation of four or more phosphorylated GC-A residues to alanine produced an enzyme that was not activated by ANP (19). In contrast, glutamate substitutions for the individual phosphorylation sites to mimic the negative charge of phosphate preserves the ability of the enzymes to transmit the NP binding signal to the catalytic domain (20, 29, 32, 33). Importantly, unphosphorylated versions of GC-A and GC-B containing glutamate substitutions for known phosphorylation sites have the same basal and NP-stimulated activities as the wildtype phosphorylated enzymes but are not inactivated by dephosphorylation (23, 29, 32).

Changes in GC-B phosphorylation regulates the resumption of meiosis in the ovarian follicle (21, 22, 34–36) as well as longitudinal bone growth (24, 37) and skeletal bone mineral density (38) in mice, but little is known about how phosphorylation of GC-A regulates physiology *in vivo*. To date, genetically modified mice examining the physiological roles of GC-A have consisted of knockout, loss of function, or transgenic overexpression, gain of function, models (5, 6, 39–45). In these mice, GC-A is either always “on” or always “off.” Here, we created a novel knock-in mouse model called GC-A$^{8E/8E}$ that globally expresses GC-A-8E in place of both wild type alleles. These mice exhibit increased and prolonged cGMP synthesis only in the presence of ANP and/or BNP, which mimics physiologic conditions. Using this model, we investigated how GC-A affects cardiac morphology and function by measuring cardiomyocyte (CM) cross-sectional area (CSA) and performing echocardiography on GC-A$^{WT/WT}$ and GC-A$^{8E/8E}$ mice of both sexes. We furthered our investigations into this process by determining if the increased NP-dependent GC-A activity observed with GC-A-8E mice resulted in a greater and more sustained reductions in the phosphorylation of the extracellular regulated kinases (ERK) 1 and 2, well-known activators of cardiac hypertrophy in mice.

## 2. MATERIALS AND METHODS

### 2.1 Animals.

GC-A$^{8E/8E}$ mice that express GC-A-8E in a global manner were created by CRISPR-Cas9 technology at the University of Connecticut Center for Mouse Genome Modification. Primer design and the overall approach to making the GC-A$^{8E/8E}$ mice is described in Supplemental Figure 1A and is based on characterization studies of rat GC-A-8E expressed in transfected cells (32). Male and female GC-A$^{WT/WT}$ and GC-A$^{8E/8E}$ mice were genotyped as shown in Supplemental Figure 1 and maintained on a C57BL/6 background as previously described (22). Mice were fed standard chow under specific-pathogen-free conditions. All mice were 12 weeks old unless otherwise indicated. Animal care and use was compliant with the University of Minnesota and University of Connecticut Institutional Animal Care and Use Committees.

### 2.2 Reagents.

Antibodies were from the following sources: anti-ERK1/2 P-thr 202 and P-tyr 204 #9101, anti-ERK1/2 #9102, anti-MEK1/2 P-ser 217 and P-ser 221 #9121, anti-MEK1/2 #9122 (Cell Signaling, Danvers, MA, USA), and anti MKP-1/DUSP1 (E-6)(Santa Cruz Biotechnology, Dallas, TX, USA). Antibodies to GC-A were generated and used as described (46). ELISA kits for cGMP and aldosterone were from ENZO Lifesciences, Inc. (Farmingdale, New York, USA). The testosterone ELISA was from Cayman Chemical (Ann Arbor, MI56t). ELISAs for mouse ANP and mouse BNP were from RayBiotech (Peachtree Corners, GA, USA). fsANP was from Anaspec (Fremont, CA, USA) as previously described (47). The mouse creatinine assay kit was from Crystal Chem (Elk Grove Village, IL, USA).

### 2.3 Guanylyl Cyclase Activity Assays.

Heart and kidney tissue were homogenized in phosphatase inhibitor buffer (PIB) at 4°C (48). Assays were performed at 37 °C in a buffer containing 25 mM HEPES, pH 7.4, 50 mM NaCl, 0.1% BSA, 0.5 mM isobutylmethylxanthine, 1 mM EDTA, 0.5 μM microcystin, 5 mM $MgCl_2$, 0.1 μg/ml creatine kinase, 5 mM creatine phosphate, 1 mM ATP, and 1 mM GTP in the absence or presence of 1 μM ANP for the indicated periods of time. Assays were terminated with 0.5 ml of 110 mM ZnOAc followed by 0.5 ml 110 mM $Na_2CO_3$, which was centrifuged to separate the GTP from cGMP. Cyclic GMP from the eluate was purified on acidified alumina columns as previously described (49). The cGMP was eluted with 3 ml of 200 mM ammonium formate and added undiluted to the ELISA assay as described (48).

### 2.4 Immunoprecipitation and western blotting of GC-A.

0.15–0.25 g of membrane protein from whole kidneys or 0.08–0.10 g of membrane protein from cardiac ventricles were prepared in 0.5 to 1.0 ml of PIB from wild type and GC-$A^{8E/8E}$ mice and immunoprecipitated with 2 μl of serum from rabbit #6326 that was immunized with a peptide corresponding to the last 17 C-terminal amino acids of rat GC-A (19). Samples were fractionated on an 8% gel by SDS-PAGE and blotted to a polyvinylidene difluoride membrane. The membrane was blocked with Odyssey LI-COR blocking buffer (Li-Cor Biosciences, Lincoln, NE) for 1 h at room temperature and then incubated overnight at 4°C with the same antiserum at a dilution of 1:10,000 in 1:1 blocking buffer/PBS with 0.1% Tween. The membrane was washed 4 × 5 min with TBST and then incubated with IRDye 680 goat anti-rabbit antibody with a dilution of 1:15,000 for 1 h at room temperature in 1:1 blocking buffer/PBST and 0.01% SDS. The membrane was washed 4 × 5 min with TBST and once with PBS before imaging on a Li-Cor infrared imaging device. The relative amount of GC-A protein was determined using NIH ImageJ software.

### 2.5 Telemetry implantation.

16-week-old male GC-$A^{WT/WT}$ and GC-$A^{8E/8E}$ mice were implanted with Data Science International Inc. (St. Paul, MN, USA) transmitters (model HD-X11) for continuous monitoring of arterial pressure and heart rate as previously described (50). The surgical area was shaved and disinfected with iodine and cleaned with 70% isopropyl alcohol. The mice were placed on a heated surgical pad and a midline back incision was made to subcutaneously implant the body of the transmitter and a second incision was made in the

interior side of the left leg to access the femoral artery for placement of the catheter of the transmitter. Mice were then allowed to recover for 1 week before telemetry data was collected during the period of 17–20 weeks of age.

### 2.6 Heart Histology.

Hearts from GC-A$^{WT/WT}$ and GC-A$^{8E/8E}$ mice were arrested in diastole with 200 μl of PBS supplemented with 60mM KCl, excised, cleaned, and weighed. Hearts were cannulated through the aorta and perfused with PBS supplemented with 60 mM KCl, followed by 4% paraformaldehyde. Fixed hearts were embedded in paraffin and then sectioned transversely at the midpoint of the ventricles. Sections were stained with wheat germ agglutinin (WGA) and DAPI, imaged at 10X magnification, and analyzed for cardiomyocyte (CM) cross sectional area (CSA) using ImageJ by averaging the area of at least 250 CMs per heart (51, 52).

### 2.7 Subcutaneous fsANP injections.

Frameshift (fs) ANP was dissolved in water at a concentration of 1 mM and frozen at −80°C until used as previously described (47). Mice were subcutaneously injected with 2 mg/kg fsANP or with an equal volume of saline as vehicle control.

### 2.8 Plasma and urine analysis.

Plasma ANP, BNP, aldosterone, testosterone, and cGMP concentrations were determined by ELISA according to the manufacturer's instructions. Plasma and urine creatinine was determined by an enzymatic assay according to manufacturer's instructions.

### 2.9 ERK analysis.

Ventricular lysates were prepared from GC-A$^{WT/WT}$ and GC-A$^{8E/8E}$ mice by homogenizing with a Polytron in ice-cold RIPA buffer containing 50 mM Tris HCl, pH 7.4, 150 mM NaCl, 1% Triton X-100, 0.5% sodium deoxycholate, 0.1% SDS, 1 mM EDTA, and 10 mM NaF with Roche (San Francisco, CA, USA) complete protease inhibitor tablet and microcystin added fresh followed by agitation for 30 min at 4°C. The lysates were then centrifuged at 14,000g for 10 minutes at 4°C and the supernatant was collected. Thirty micrograms of ventricular lysates were fractionated on a 10% gel by SDS-PAGE and transferred for 1 h at 100 V to a polyvinylidene difluoride membrane. The membrane was blocked with LI-COR blocking buffer for 1 h at room temperature and then incubated overnight at 4°C with primary antibody. The membrane was washed 3 × 5 min with TBST and then incubated with IRDye 680 goat anti-rabbit antibody with a dilution of 1:15,000 for 1 h at room temperature in LI-COR blocking buffer. The membrane was washed 3 × 5 min with TBST and then once with TBS and then visualized and quantified on a Li-Cor infrared imaging device.

### 2.10 Echocardiography.

Echocardiography was performed using the Vevo 2100 (FujiFilm VisualSonics Inc. Toronto, ON, Canada) with a MS550 transducer on anesthetized mice that were gently restrained in the supine position on the prewarmed monitoring pad. Echocardiographic images were captured as mice were recovering from anesthesia to achieve a heart rate (HR) of 400

– 500 bpm. Parasternal long axis M-mode images of the left ventricle were captured to measure left ventricular posterior wall thicknesses during systole (LVPW;s) and diastole (LVPW;d), left ventricular internal diameters (LVID;s and LVID;d), left ventricular end systolic volume (ESV: (7.0/(2.4 + LVIDs))*$LVIDs^3$) and end diastolic volume (EDV: (7.0/(2.4 + LVIDd))*$LVIDd^3$), fractional shortening (FS: 100*((LVIDd – LVIDs)/LVIDd)), ejection fraction (EF: 100*((EDV – ESV)/EDV)), stroke volume (SV: EDV – ESV), and cardiac output (CO: SV*HR). Pulsed-wave Doppler images of the aortic arch were recorded to measure peak aortic velocity (AoV). Pulsed-wave Doppler images of the apical four-chamber view were taken to measure mitral flow velocities (E wave and A wave to calculate E/A ratio).

### 2.11 Statistics.

Statistics and graphs were generated with Prism 9 software (GraphPad Software, La Jolla, CA, USA). p-values were obtained using either an unpaired, two-tailed student's t-test, Mann-Whitney test (panels A and B of figure 4), or two-way ANOVA with or without repeated-measures followed by Turkey's post-hoc test where $p \leq 0.05$ was considered significant.

## 3. RESULTS

### 3.1 Generation and validation of the GC-$A^{8E/8E}$ mice.

Cell culture studies indicated that a rat GC-A variant containing glutamate substitutions for the eight confirmed phosphorylation sites is activated by ANP like the phosphorylated wild type receptor (32). Here, glutamates were substituted for Ser-473, Ser-487, Ser-497, Thr-500, Ser-502, Ser-506, Ser-510 and Thr-513 using amino acid numbering based on the rat cDNA as initially described by Otto et al. (32). All substitutions were confirmed by DNA sequencing (Supplemental Fig. 1B). PCR-based genotyping indicated that heterozygous breeding produced the GC-$A^{WT/WT}$, GC-$A^{8E/+}$ and GC-$A^{8E/8E}$ lines at the expected mendelian ratios (Supplemental Fig. 1C). At 12 weeks of age, there was no difference in body weight between the GC-$A^{WT/WT}$ and GC-$A^{8E/8E}$ mice. Additionally, no differences in the mass of livers, lungs, or kidneys that express high levels of GC-A were observed between the GC-$A^{WT/WT}$ and GC-$A^{8E/8E}$ mice (Supplemental Table 1A). No obvious differences were observed in fertility between wild type or mutant mice as well.

### 3.2 Plasma cGMP concentrations are elevated in GC-$A^{8E/8E}$ mice.

Plasma was isolated between 4:00PM and 6:00PM from male and female GC-$A^{WT/WT}$ and GC-$A^{8E/8E}$ mice and analyzed for ANP, BNP and cGMP by ELISA. Plasma ANP and BNP concentrations did not differ between GC-$A^{WT/WT}$ and GC-$A^{8E/8E}$ mice of either sex (Fig. 1A–D). However, cGMP levels were elevated 95.1% and 80.1% in male and female GC-$A^{8E/8E}$ mice, respectively, compared to their wild type littermates (Fig. 1E and F).

### 3.3 GC-$A^{8E/8E}$ mice have greater ANP-dependent guanylyl cyclase activity but not GC-A protein.

Membranes from cardiac ventricles and whole kidneys of male and female mice of both genetic lines were assayed for GC-A activity in the presence of saturating amounts of ANP

as a function of time. As anticipated, both male and female GC-A$^{8E/8E}$ mice had two to four times more ANP-dependent GC-A activity in these tissues compared to GC-A$^{WT/WT}$ mice (Fig. 2A and B). The difference in activity was not explained by variances in protein concentrations because GC-A protein levels measured by sequential immunoprecipitation-western blot analysis from hearts and kidneys were similar between GC-A$^{WT/WT}$ and GC-A$^{8E/8E}$ mice (Fig. 2C and D). Plausible explanations for the increased ANP-dependent GC activity in tissues from the GC-A$^{8E/8E}$ mice are that more of the translated GC-A protein from the GC-A$^{8E/8E}$ mice is active since it does not require post-translational phosphorylation and/or a significant amount of the WT GC-A protein is not completely phosphorylated at any one time (19). Unexpectedly, both GC-A$^{WT/WT}$ and GC-A$^{8E/8E}$ female mice had approximately three-fold more ventricular ANP-dependent GC-A activity than males of the same genotype, whereas renal GC-A activity was similar between sexes. Again, these sex-dependent differences in cardiac activity were not explained by variances in GC-A protein concentrations based on western blots (Fig. 2C).

### 3.4 Blood pressure is unchanged between male GC-A$^{WT/WT}$ and GC-A$^{8E/8E}$ mice.

To investigate potential blood pressure differences between the GC-A$^{WT/WT}$ and GC-A$^{8E/8E}$ mice, 16-week-old male mice of both lines were implanted with telemetry sensors that monitor blood pressure and heart rate continuously (50). One week after sensor implant surgery, the mice were sequentially fed diets containing varying NaCl content for approximately one week during the 17-week-old to 20-week-old time period, which resulted in a 40-fold range in NaCl intake. However, regardless of the dietary salt content, neither mean arterial pressure (MAP) (Fig. 3A) nor heart rate (Fig. 3B) differed between mice of the two genotypes.

### 3.5 The release of creatinine into the urine is increased in male GC-A$^{8E/8E}$ mice.

To determine if renal function was changed in the mutant mice, we measured plasma and urine creatinine concentrations. Plasma creatinine levels for the male GC-A$^{WT/WT}$ mice were about 0.2 mg/dL, which is consistent with previously reported mouse plasma creatinine levels (Fig. 4A)(53). In contrast, creatinine levels from several of the male GC-A$^{8E/8E}$ mice were below the limit of detection of our assay. This is not unexpected since in the absence of renal dysfunction, plasma creatinine is low. Given that plasma creatinine levels in 6 of the 10 male GC-A$^{8E/8E}$ mice were below the assay's level of detection, the most conservative analysis of this data is to assign values for the samples that were below the last standard on the curve to the lowest value that was on the curve and use the nonparametric, Mann-Whitney test to assess statistical differences. When applied, this approach yielded a statistically significant decrease ($p = 0.0018$) in male GC-A$^{8E/8E}$ creatinine concentrations compared to the GC-A$^{WT/WT}$ mice. Creatinine levels in urine were also measured in male mice of both genotypes and found to be significantly elevated in the male GC-A$^{8E/8E}$ mice (Fig. 4C). In contrast, no differences in urine creatinine concentrations were observed between the female WT and mutant mice. Taken together, these data provide strong evidence that the male GC-A$^{8E/8E}$ mice release more creatinine into the urine than GC-A$^{WT/WT}$ mice, which is consistent with the well-known ability of GC-A to increase the glomerular filtration rate (54).

### 3.6 Male GC-A$^{8E/8E}$ mice have smaller hearts and cardiomyocytes.

Hearts from GC-A$^{8E/8E}$ male mice were 8% smaller by weight (Fig. 5A and C), but body weights were not different (Fig. 5D), which resulted in heart weight-to-body weight ratios that were 12% lower compared to GC-A$^{WT/WT}$ male mice (Fig. 5E). No differences were observed between the female GC-A$^{8E/8E}$ and GC-A$^{WT/WT}$ mice (Fig. 5B and F–H). To further investigate the reduced cardiac hypertrophy in males, ventricles were sectioned and stained to determine the cross-sectional area (CSA) of individual CMs (Fig. 5I). Male GC-A$^{8E/8E}$ mice had a 14% decrease in CM CSA compared to the GC-A$^{WT/WT}$ male mice (Fig. 5J), consistent with the known cardiac anti-hypertrophic effects of GC-A (6, 10). Hence, this reduction in CM CSA accounts for the reduction in heart size in the GC-A$^{8E/8E}$ male mice. Consistent with the lack of differences in female heart size, CM CSA did not differ in hearts from female GC-A$^{8E/8E}$ or GC-A$^{WT/WT}$ mice (Fig. 5K).

### 3.7 Plasma aldosterone levels are elevated in male, but not female, GC-A$^{8E/8E}$ mice.

Because mice with mutations that increase plasma aldosterone concentrations have higher blood pressure (55), and the GC-A$^{8E/8E}$ mice do not have reduced blood pressure as expected due to the increased GC-A activity, we measured aldosterone levels in our GC-A$^{WT/WT}$ and GC-A$^{8E/8E}$ mice that were fed normal chow diets with no added NaCl. Aldosterone concentrations were 78% higher in male GC-A$^{8E/8E}$ mice (557.8 pg/ml) compared to male GC-A$^{WT/WT}$ mice (312.5 pg/ml) (Fig. 6A). In contrast, no significant difference in plasma aldosterone concentrations was observed between the female GC-A$^{WT/WT}$ (264.8 pg/ml) and GC-A$^{8E/8E}$ (249.5 pg/ml) mice (Fig. 6B).

### 3.8 Plasma testosterone levels are elevated in male and female GC-A$^{8E/8E}$ mice.

Previous reports correlated changes in cardiac hypertrophy and hypertension in genetic models with increased GC-A-dependent blood testosterone concentrations (56, 57). Therefore, we measured plasma testosterone levels in male and female GC-A$^{WT/WT}$ and GC-A$^{8E/8E}$ mice. We found that male GC-A$^{WT/WT}$ mice had plasma testosterone levels of 3.68 ng/ml compared to 5.4 ng/ml for male GC-A$^{8E/8E}$ mice, whereas female GC-A$^{WT/WT}$ mice had plasma testosterone levels of 0.08 ng/ml compared to 0.12 ng/ml for female GC-A$^{8E/8E}$ mice. For both sexes, plasma testosterone levels were significantly elevated in the mutant mice (Fig. 6C and D).

### 3.9 Analysis of cardiac ERK phosphorylation in male GC-A$^{8E/8E}$ mice.

Cardiac hypertrophy is positively regulated by the ERK1/2 pathway (58–60), and ANP and BNP have been shown to decrease ERK1/2 phosphorylation in cultured cells (61–63). Therefore, we investigated whether ERK1/2 activity is reduced in male GC-A$^{8E/8E}$ mice. Hearts were removed from male GC-A$^{8E/8E}$ and GC-A$^{WT/WT}$ mice and ventricular extracts were fractionated by SDS-PAGE and transferred to a PVDF membrane. Western blots were probed with an antibody against phosphorylated ERK1/2, then stripped and re-probed with an antibody against ERK1/2 protein and GAPDH. The amount of phospho-ERK and total ERK protein were quantified and used to determine the stoichiometry of ERK1/2 phosphorylation. Although ventricular ERK1/2 phosphorylation trended lower in extracts from the GC-A$^{8E/8E}$ mice, the difference was not statistically significant (Supplemental Fig.

2A and B). We also measured protein expression of MKP-1/DUSP1, a phosphatase known to reduce ERK1/2 phosphorylation, but observed no significant differences (Supplemental Fig. 2C). We then examined ERK1/2 phosphorylation in younger, 4-week-old mice, and again found that ERK1/2 phosphorylation trended lower in the male GC-A$^{8E/8E}$ mice, but that the decrease was not statistically significantly different from the wild type mice (Supplemental Fig. 3).

### 3.10 fsANP injections result in higher and more sustained plasma cGMP concentrations in male, but not female, GC-A$^{8E/8E}$ mice.

Since GC-A activity is not increased without NP stimulation in our GC-A$^{8E/8E}$ model (32), we subcutaneously injected mice with saline or fsANP, a C-terminally extended, long-lived ANP analog (47, 64) as performed by Chen et al. in rats (65). Plasma cGMP concentrations were elevated more than three-fold 15 minutes after injection of fsANP in the GC-A$^{WT/WT}$ mice and declined to basal levels by 60 minutes. Saline did not increase plasma cGMP concentrations at any time period (Fig. 7A). Injections of fsANP into male GC-A$^{WT/WT}$ mice and GC-A$^{8E/8E}$ mice resulted in similar plasma cGMP elevations at 5 minutes. However, while cGMP concentrations peaked 10 to 15 minutes after fsANP injection for the male GC-A$^{WT/WT}$ mice, plasma cGMP concentrations in the male GC-A$^{8E/8E}$ mice continued to climb for 20 minutes, at which point the plasma cGMP concentrations plateaued (Fig. 7B). Elevated plasma cGMP concentrations in the GC-A$^{8E/8E}$ mice are consistent with the GC-A$^{8E/8E}$ mice not undergoing dephosphorylation-dependent homologous desensitization (14, 16, 29, 32, 66, 67). As a result of the prolonged cGMP production in the GC-A$^{8E/8E}$ mice, plasma cGMP concentrations were more than two-fold higher in the male GC-A$^{8E/8E}$ mice compared to male GC-A$^{WT/WT}$ mice during the 15-to-30-minute time period. In contrast, little difference was observed between fsANP-dependent plasma cGMP elevations in female GC-A$^{WT/WT}$ and GC-A$^{8E/8E}$ mice (Fig. 7C).

### 3.11 fsANP injection decreases plasma aldosterone similarly in male GC-A$^{8E/8E}$ and GC-A$^{WT/WT}$ mice at 15, but not at 60 minutes.

Plasma aldosterone concentrations from both male GC-A$^{WT/WT}$ and GC-A$^{8E/8E}$ mice taken 15 minutes after subcutaneous injection with fsANP were reduced to similar levels (WT fsANP: 53% of vehicle, 8E fsANP: 62% of vehicle)(Supplemental Fig. 4A), which is consistent with previous reports showing that ANP decreases plasma aldosterone concentrations (68). However, while plasma aldosterone concentrations from male GC-A$^{WT/WT}$ mice taken 1 hour after subcutaneous injection with fsANP were back to vehicle control levels, plasma aldosterone levels from GC-A$^{8E/8E}$ mice were significantly elevated above vehicle control levels (Supplemental Fig. 4B). These data are consistent with a dysregulation of the GC-A/aldosterone regulatory axis in the GC-A$^{8E/8E}$ mice.

### 3.12 fsANP injection decreases ventricular ERK1/2 phosphorylation to a greater extent and for a longer period in GC-A$^{8E/8E}$ compared to GC-A$^{WT/WT}$ mice.

ERK1/2 regulatory phosphorylation was determined by Western blot in ventricular extracts from male GC-A$^{WT/WT}$ and male GC-A$^{8E/8E}$ mice 5-, 15-, 30-, and 60-minutes after injection with fsANP (Fig. 8A–B and Supplemental Fig. 5A–H). The phospho-ERK/total-ERK values were normalized to mean values from saline-injected control mice and plotted

as a function of time after injection (Fig. 8D). For the male GC-A$^{WT/WT}$ mice, the maximum decrease in ERK1/2 activity was 57%, which occurred at the earliest time period of 5-minutes and recovered to 89% of the unstimulated control value by the 60-minute timepoint. In contrast, cardiac ERK1/2 activities in the male GC-A$^{8E/8E}$ mice reached a nadir of 40% 30 minutes after the fsANP injection, which remained significantly depressed at 57% of the control value 60-minutes after the fsANP injection. Importantly, no difference in ERK1/2 phosphorylation in ventricular extracts from female GC-A$^{8E/8E}$ and GC-A$^{WT/WT}$ mice was observed 30 minutes after fsANP injection (Fig. 8C). Finally, no change in MEK activity in these same cardiac extracts was detected (Supplemental Fig. 6). Together, these data indicate that acute NP activation of GC-A reduces ERK1/2 activity in cardiac ventricles to a greater extent and for a longer period of time in male GC-A$^{8E/8E}$ compared to male GC-A$^{WT/WT}$ mice.

### 3.13 Male GC-A$^{8E/8E}$ mice have improved systolic function.

To determine if increased NP-dependent GC-A activity affects cardiac function, we performed echocardiography on male and female mice of both lines (Fig. 9 and Supplemental Table 1B). Despite their smaller hearts, male GC-A$^{8E/8E}$ mice had increased ejection fractions and fractional shortening compared to the male GC-A$^{WT/WT}$ mice (Fig. 9A and Supplemental Table 1B). End systolic volume was also decreased in the mutant male mice (Fig. 9B). However, the E/A ratio did not differ between the wild type and mutant mice, indicating that the GC-A$^{8E/8E}$ male mice had normal diastolic function (Fig. 9D). In contrast, none of the measured heart functions were significantly different between the mutant and wild type female mice (Fig. 9E–H and Supplemental Table 1B). Together, these data indicate that the male GC-A$^{8E/8E}$ mice have improved systolic function despite having smaller hearts.

## 4. DISCUSSION

Using a novel mouse model that exhibits increased GC-A activity only in the presence of endogenous levels of ANP and/or BNP, we investigated how prevention of GC-A dephosphorylation regulates physiology in a live animal. The GC-A$^{8E/8E}$ mice have greater and longer lasting NP-dependent GC activity, but normal basal activity, which provides a new perspective for examining the effects of increased GC-A activity *in vivo*. This increased GC-A activity was associated with decreased heart size in male, but not female, GC-A$^{8E/8E}$ mice, which is consistent with more severe cardiac hypertrophy observed in male compared to female GC-A$^{-/-}$ mice. (6). The smaller heart phenotype was not explained by changes in blood pressure since the blood pressure between male GC-A$^{WT/WT}$ and GC-A$^{8E/8E}$ mice did not differ over a 40-fold change in dietary NaCl content. These data are harmonious with reports demonstrating pressure-independent effects of GC-A on cardiac hypertrophy (8–10). Microscopy studies indicated that the decreased heart size in male GC-A$^{8E/8E}$ mice was explained by reduced CM CSA, which is in agreement with increased CM CSA in male GC-A$^{-/-}$ mice (6). Importantly, male but not female GC-A$^{8E/8E}$ mice had improved systolic function compared to GC-A$^{WT/WT}$ mice, despite having smaller hearts. These data are consistent with that of mice expressing four GC-A alleles (Npr1$^{++/++}$) that had reduced heart weight to body weight ratios and increased fractional shortening (69) as well as with

GC-A$^{-/-}$ mice that had cardiac hypertrophy and increased left ventricular end diastolic and systolic dimensions (6). Hence, the totality of data indicate that gain of function GC-A models result in smaller male hearts with improved systolic function, whereas loss of function models result in larger male hearts with reduced systolic function.

Unexpectedly, there was no significant difference in blood pressure between male GC-A$^{8E/8E}$ and GC-A$^{WT/WT}$ mice, even when measured over a wide range of salt intake. The GC-A knockout mice have chronically elevated blood pressure that is unresponsive to changes in salt-intake (5, 6), whereas the Npr1$^{++/++}$ mice that express four GC-A alleles exhibit increased GC-A activity and are hypotensive (40). Increased urinary creatinine indicates that at least one known renal function of GC-A is elevated in the GC-A$^{8E/8E}$ mice as expected. One potential explanation for the lack of reduction in blood pressure in the male GC-A$^{8E/8E}$ mice is that the elevated plasma aldosterone concentrations observed in the GC-A$^{8E/8E}$ mice may compensate for the increased GC-A activity to normalize blood pressure. Why aldosterone was unchanged in the original GC-A$^{-/-}$ mice (5) and increased in the same mice many years later is not known (70).

A previous study reported that mice with increasing numbers of GC-A alleles have proportionally increased GC-A activity, proportionally increased blood testosterone levels, and proportionally decreased blood pressure (57). Hence, it was suggested that the GC-A dependent increases in testosterone levels contribute to the hypotension observed in mice with increased GC-A activity. However, in our model, where GC-A activity is only increased in response to natural ligand activation, we observed no change in blood pressure despite significant increases in blood testosterone levels in male mice. Additionally, Li et al suggested that male mice exhibit more cardiac hypertrophy than female mice because they have higher testosterone levels (56). However, in our model where the male mice exhibit increased GC-A activity and testosterone levels, these mice display reduced cardiac hypertrophy. Similarly, the female GC-A$^{8E/8E}$ mice have 48% higher serum testosterone levels as the female GC-A$^{WT/WT}$ mice but show no signs of hypertrophy. Hence, increased testosterone levels are neither associated with hypotension in male mice nor cardiac hypertrophy in mice of either sex in our GC-A$^{8E/8E}$ model.

Cyclic GMP stimulated by NPs, but not nitric oxide, counteracts cardiac hypertrophy in murine knockout hypertension models by directly acting on CMs (5, 8–10, 71, 72), and reductions in NP-dependent cGMP concentrations by phosphodiesterase 9A result in pathologic cardiac hypertrophy (73). Significantly, GC-A has been shown to decrease ERK1/2 activity in cultured cells by many investigators through a mechanism that is usually mimicked by cGMP analogs and requires protein kinase G (61–63, 74, 75), although Hofmann and colleagues have shown that protein kinase G I is not required for reductions in transaortic constriction (TAC)-dependent or angiotensin II-dependent cardiac hypertrophy in mice (76–78).

Cardiac hypertrophy can be physiologic as occurs during development and exercise, or pathologic as occurs with hypertension and chemotherapy (60, 79). ERK1/2 activation is more closely associated with physiologic as opposed to pathologic cardiac hypertrophy (79). Genetic studies involving ERK1$^{-/-}$ and ERK2$^{+/-}$ mice, or studies using mice overexpressing

dual specificity phosphatase 6 that dephosphorylates and inactivates ERK1/2 (60, 79), suggest that increased ERK1/2 activity is not required for pathological cardiac hypertrophy (80, 81).

Regarding the physiologic consequences of GC-A inhibition of ERK1/2 in the heart, CM-specific transgenic overexpression of MEK-1, the direct upstream activator of ERK1/2, induces physiologic hypertrophy (82) and attenuates ischemic injury (83, 84), whereas ERK1$^{-/-}$ and ERK2$^{+/-}$ mice are more susceptible to ischemic injury (82). Here, the reduced activation of ERK1/2 in hearts from the GC-A$^{8E/8E}$ mice is mechanistically consistent with decreased hypertrophic growth observed in these mice with development. Moreover, physiologic cardiac hypertrophy associated with lactation was exaggerated in GC-A$^{-/-}$ mice and correlated with increased cardiac ERK1/2 phosphorylation and activity (70). Conversely, in GC-A$^{-/-}$ mice, exaggeration of pathologic hypertrophy post-TAC was not dependent on ERK1/2 activity (9, 11). Finally, the ability of ANP to block phenylephrine-dependent increases in neonatal rat CM CSA was shown to require increased, not decreased, ERK1/2 activity, which differs from our model (85). Regardless, the majority of data indicate that GC-A-dependent CM ERK1/2 inhibition is context dependent, such that reduced activation of ERK1/2 in GC-A$^{8E/8E}$ mice attenuates developmental hypertrophy but is not required for pathologic hypertrophy in the GC-A$^{-/-}$ mice post-TAC. Hence, the mechanism that GC-A uses to regulate cardiac hypertrophy in development as demonstrated by the GC-A$^{8E/8E}$ mice is distinct from the mechanism associated with pathologic cardiac hypertrophy as originally suggested by Scott et al. (12).

Surprisingly, we observed much greater GC-A activity in ventricular membranes from both female GC-A$^{8E/8E}$ and GC-A$^{WT/WT}$ mice compared to membranes from male mice of each genotype. To our knowledge, this is the first demonstration of a sex difference in cardiac GC-A activity. One explanation for why only male GC-A$^{8E/8E}$ mice have smaller hearts is that the ANP-dependent GC-A activity in the female GC-A$^{WT/WT}$ ventricles is elevated above the threshold level required to inhibit the CM ERK1/2 pathway. In contrast, GC activity in the male wild type mice is below this threshold. Thus, the increased activity observed in the male GC-A$^{8E/8E}$ mice is now high enough to inhibit the CM ERK1/2 pathway. In contrast, GC-A activity in the female GC-A$^{WT/WT}$ mice is already sufficiently elevated to inhibit the CM ERK1/2 pathway, and therefore, the additional GC-A activity observed in the female GC-A$^{8E/8E}$ mice provides no additional benefit. Interestingly, the increased GC-A activity in female ventricles may explain the cardioprotective effects of estrogen on CMs mediated by GC-A (86, 87). These studies determined that estrogen increases ANP concentrations, while our data demonstrates that GC-A activity is much higher in ventricles from female mice. The increases in both ANP and GC-A activity in murine female ventricles would increase cGMP concentrations in CMs, which is a known inhibitor of cardiac hypertrophy (9, 10, 61).

In conclusion, we developed a novel mouse model to study the physiologic consequences of NP-dependent, but phosphorylation-independent, activation of GC-A *in vivo*. Using this model and subcutaneous injections of a long-lived ANP analog, we determined that preventing dephosphorylation-dependent inactivation of GC-A has measurable, physiological consequences. The male GC-A$^{8E/8E}$ mice have smaller hearts due to

reduced CM hypertrophy, despite exhibiting elevated plasma aldosterone and testosterone concentrations. Activation of GC-A with fsANP produced greater and more sustained plasma cGMP elevations, which correlated with larger and longer reductions of cardiac ERK1/2 phosphorylation in male GC-A$^{8E/8E}$ mice. Thus, increased cardiac GC-A activity reduces CM size in male GC-A$^{8E/8E}$ mice by decreasing ventricular ERK1/2 activity, a well-known regulator of cardiac hypertrophy. Finally, we note that GC-A$^{8E/8E}$ mice not only have less cardiac phospho-ERK1/2 protein, but they also have elevated plasma aldosterone levels compared to the wild type mice. Importantly, these two differences are most apparent at longer time periods after injection with fsANP, which is consistent with the disparities being mediated by the prolonged GC activity of the GC-A-8E protein endogenously expressed in the GC-A$^{8E/8E}$ mice.

## Supplementary Material

Refer to Web version on PubMed Central for supplementary material.

## ACKNOWLDEGMENTS

The authors thank Dr. Laurinda Jaffe for sharing the GC-A-8E mice as well as for providing helpful comments on multiple versions of this manuscript. We thank Drs. Michael Kalwat and Melanie Cobb for helpful advice regarding ERK1/2 Western blots. We acknowledge the Phenotyping Core at the University of Minnesota for surgical and technical expertise on data acquisition using telemetry devices. We thank Dr. Pilar Ariza-Guzman for the implantation and monitoring of the telemetry devices. The authors also acknowledge the University of Minnesota Imaging Centers for advice and support for echocardiography studies.

**Funding Sources:**

This work was supported by National Institutes of Health Grant R01GM098309, a University of Minnesota Foundation Bridge Grant, a University of Minnesota-Mayo Clinic Partnership grant, a University of Minnesota Academic Health Center Faculty Research and Development Grant and Grants from the Fund for Science and the Hormone Receptor Fund to LRP. NIHT32DK007203 Grant supported JWR. NIH R01HL130099 and NIH R01HL152215 to TDO also funded portions of this work.

## Abbreviations:

| | |
|---|---|
| **ANP** | atrial natriuretic peptide |
| **ANOVA** | analysis of variance |
| **BNP** | b-type natriuretic peptide |
| **CM** | cardiomyocyte |
| **Cas9** | CRISPR-associated protein 9 |
| **CRISPR** | clustered regularly interspaced short palindromic repeats |
| **CSA** | cross sectional area |
| **cGMP** | cyclic guanosine monophosphate |
| **DAPI** | 4’,6-diamidino-2-phenylindole |
| **ERK** | extracellular regulated kinase |

| | |
|---|---|
| **fs** | frameshift |
| **GC** | guanylyl cyclase |
| **IR** | infrared |
| **MAP** | mean arterial pressure |
| **MEK** | ERK kinase |
| **NP** | natriuretic peptide |
| **PIB** | phosphatase inhibitor buffer |
| **SEM** | standard error of the mean |
| **TAC** | transverse aortic constriction |
| **WGA** | wheat germ agglutinin |

## REFERENCES


1. Potter LR, Abbey-Hosch S, and Dickey DM (2006) Natriuretic peptides, their receptors, and cyclic guanosine monophosphate-dependent signaling functions. Endocr Rev 27, 47–72 [PubMed: 16291870]
2. Kuhn M (2016) Molecular Physiology of Membrane Guanylyl Cyclase Receptors. Physiol Rev 96, 751–804 [PubMed: 27030537]
3. Kishimoto I, Dubois SK, and Garbers DL (1996) The heart communicates with the kidney exclusively through the guanylyl cyclase-A receptor: acute handling of sodium and water in response to volume expansion. Proc Natl Acad Sci U S A 93, 6215–6219 [PubMed: 8650246]
4. Lopez MJ, Garbers DL, and Kuhn M (1997) The guanylyl cyclase-deficient mouse defines differential pathways of natriuretic peptide signaling. J Biol Chem 272, 23064–23068 [PubMed: 9287305]
5. Lopez MJ, Wong SK, Kishimoto I, Dubois S, Mach V, Friesen J, Garbers DL, and Beuve A (1995) Salt-resistant hypertension in mice lacking the guanylyl cyclase-A receptor for atrial natriuretic peptide. Nature 378, 65–68 [PubMed: 7477288]
6. Oliver PM, Fox JE, Kim R, Rockman HA, Kim HS, Reddick RL, Pandey KN, Milgram SL, Smithies O, and Maeda N (1997) Hypertension, cardiac hypertrophy, and sudden death in mice lacking natriuretic peptide receptor A. Proc Natl Acad Sci U S A 94, 14730–14735 [PubMed: 9405681]
7. Matsukawa N, Grzesik WJ, Takahashi N, Pandey KN, Pang S, Yamauchi M, and Smithies O (1999) The natriuretic peptide clearance receptor locally modulates the physiological effects of the natriuretic peptide system. Proc Natl Acad Sci U S A 96, 7403–7408. [PubMed: 10377427]
8. Holtwick R, Van Eickels M, Skryabin BV, Baba HA, Bubikat A, Begrow F, Schneider MD, Garbers DL, and Kuhn M (2003) Pressure-independent cardiac hypertrophy in mice with cardiomyocyte-restricted inactivation of the atrial natriuretic peptide receptor guanylyl cyclase-A. J Clin Invest 111, 1399–1407 [PubMed: 12727932]
9. Knowles JW, Esposito G, Mao L, Hagaman JR, Fox JE, Smithies O, Rockman HA, and Maeda N (2001) Pressure-independent enhancement of cardiac hypertrophy in natriuretic peptide receptor A-deficient mice. J Clin Invest 107, 975–984 [PubMed: 11306601]
10. Kishimoto I, Rossi K, and Garbers DL (2001) A genetic model provides evidence that the receptor for atrial natriuretic peptide (guanylyl cyclase-A) inhibits cardiac ventricular myocyte hypertrophy. Proc Natl Acad Sci U S A 98, 2703–2706. [PubMed: 11226303]
11. Li Y, Kishimoto I, Saito Y, Harada M, Kuwahara K, Izumi T, Takahashi N, Kawakami R, Tanimoto K, Nakagawa Y, Nakanishi M, Adachi Y, Garbers DL, Fukamizu A, and Nakao K (2002) Guanylyl

cyclase-A inhibits angiotensin II type 1A receptor-mediated cardiac remodeling, an endogenous protective mechanism in the heart. Circulation 106, 1722–1728 [PubMed: 12270869]

12. Scott NJ, Ellmers LJ, Lainchbury JG, Maeda N, Smithies O, Richards AM, and Cameron VA (2009) Influence of natriuretic peptide receptor-1 on survival and cardiac hypertrophy during development. Biochim Biophys Acta 1792, 1175–1184 [PubMed: 19782130]
13. Schulz S, Singh S, Bellet RA, Singh G, Tubb DJ, Chin H, and Garbers DL (1989) The primary structure of a plasma membrane guanylate cyclase demonstrates diversity within this new receptor family. Cell 58, 1155–1162 [PubMed: 2570641]
14. Potter LR, and Garbers DL (1992) Dephosphorylation of the guanylyl cyclase-A receptor causes desensitization. The Journal of biological chemistry 267, 14531–14534 [PubMed: 1353076]
15. Potter LR (1998) Phosphorylation-dependent regulation of the guanylyl cyclase-linked natriuretic peptide receptor B: dephosphorylation is a mechanism of desensitization. Biochemistry 37, 2422–2429 [PubMed: 9485390]
16. Joubert S, Labrecque J, and De Lean A (2001) Reduced activity of the npr-a kinase triggers dephosphorylation and homologous desensitization of the receptor. Biochemistry 40, 11096–11105. [PubMed: 11551207]
17. Schroter J, Zahedi RP, Hartmann M, Gassner B, Gazinski A, Waschke J, Sickmann A, and Kuhn M (2010) Homologous desensitization of guanylyl cyclase A, the receptor for atrial natriuretic peptide, is associated with a complex phosphorylation pattern. FEBS J 277, 2440–2453 [PubMed: 20456499]
18. Potter LR, and Hunter T (1998) Identification and characterization of the major phosphorylation sites of the B-type natriuretic peptide receptor. The Journal of biological chemistry 273, 15533–15539 [PubMed: 9624142]
19. Potter LR, and Hunter T (1998) Phosphorylation of the kinase homology domain is essential for activation of the A-type natriuretic peptide receptor. Molecular and cellular biology 18, 2164–2172 [PubMed: 9528788]
20. Potter LR, and Hunter T (1999) A constitutively “phosphorylated” guanylyl cyclase-linked atrial natriuretic peptide receptor mutant is resistant to desensitization. Molecular biology of the cell 10, 1811–1820 [PubMed: 10359598]
21. Egbert JR, Shuhaibar LC, Edmund AB, Van Helden DA, Robinson JW, Uliasz TF, Baena V, Geerts A, Wunder F, Potter LR, and Jaffe LA (2014) Dephosphorylation and inactivation of NPR2 guanylyl cyclase in granulosa cells contributes to the LH-induced decrease in cGMP that causes resumption of meiosis in rat oocytes. Development 141, 3594–3604 [PubMed: 25183874]
22. Shuhaibar LC, Egbert JR, Edmund AB, Uliasz TF, Dickey DM, Yee SP, Potter LR, and Jaffe LA (2016) Dephosphorylation of juxtamembrane serines and threonines of the NPR2 guanylyl cyclase is required for rapid resumption of oocyte meiosis in response to luteinizing hormone. Dev Biol 409, 194–201 [PubMed: 26522847]
23. Robinson JW, Egbert JR, Davydova J, Schmidt H, Jaffe LA, and Potter LR (2017) Dephosphorylation is the mechanism of fibroblast growth factor inhibition of guanylyl cyclase-B. Cell Signal 40, 222–229 [PubMed: 28964968]
24. Shuhaibar LC, Robinson JW, Vigone G, Shuhaibar NP, Egbert JR, Baena V, Uliasz TF, Kaback D, Yee SP, Feil R, Fisher MC, Dealy CN, Potter LR, and Jaffe LA (2017) Dephosphorylation of the NPR2 guanylyl cyclase contributes to inhibition of bone growth by fibroblast growth factor. Elife 6
25. Haneda M, Kikkawa R, Maeda S, Togawa M, Koya D, Horide N, Kajiwara N, and Shigeta Y (1991) Dual mechanism of angiotensin II inhibits ANP-induced mesangial cGMP accumulation. Kidney Int 40, 188–194 [PubMed: 1719265]
26. Smith JB, and Lincoln TM (1987) Angiotensin decreases cyclic GMP accumulation produced by atrial natriuretic factor. Am J Physiol 253, C147–150 [PubMed: 2440311]
27. Potter LR, and Garbers DL (1994) Protein kinase C-dependent desensitization of the atrial natriuretic peptide receptor is mediated by dephosphorylation. The Journal of biological chemistry 269, 14636–14642 [PubMed: 7910166]
28. Yoder AR, Stone MD, Griffin TJ, and Potter LR (2010) Mass spectrometric identification of phosphorylation sites in guanylyl cyclase a and B. Biochemistry 49, 10137–10145 [PubMed: 20977274]

29. Yoder AR, Robinson JW, Dickey DM, Andersland J, Rose BA, Stone MD, Griffin TJ, and Potter LR (2012) A Functional Screen Provides Evidence for a Conserved, Regulatory, Juxtamembrane Phosphorylation Site in Guanylyl Cyclase A and B. PLoS ONE 7, e36747 [PubMed: 22590601]
30. Bereta G, Wang B, Kiser PD, Baehr W, Jang GF, and Palczewski K (2010) A functional kinase homology domain is essential for the activity of photoreceptor guanylate cyclase 1. J Biol Chem 285, 1899–1908 [PubMed: 19901021]
31. Pichlo M, Bungert-Plumke S, Weyand I, Seifert R, Bonigk W, Strunker T, Kashikar ND, Goodwin N, Muller A, Pelzer P, Van Q, Enderlein J, Klemm C, Krause E, Trotschel C, Poetsch A, Kremmer E, Kaupp UB, Korschen HG, and Collienne U (2014) High density and ligand affinity confer ultrasensitive signal detection by a guanylyl cyclase chemoreceptor. J Cell Biol 206, 541–557 [PubMed: 25135936]
32. Otto NM, McDowell WG, Dickey DM, and Potter LR (2017) A Glutamate-Substituted Mutant Mimics the Phosphorylated and Active Form of Guanylyl Cyclase-A. Mol Pharmacol 92, 67–74 [PubMed: 28416574]
33. Potter LR, and Hunter T (1999) A constitutively "phosphorylated" guanylyl cyclase-linked atrial natriuretic peptide receptor mutant is resistant to desensitization. Mol Biol Cell 10, 1811–1820 [PubMed: 10359598]
34. Robinson JW, Zhang M, Shuhaibar LC, Norris RP, Geerts A, Wunder F, Eppig JJ, Potter LR, and Jaffe LA (2012) Luteinizing hormone reduces the activity of the NPR2 guanylyl cyclase in mouse ovarian follicles, contributing to the cyclic GMP decrease that promotes resumption of meiosis in oocytes. Dev Biol 366, 308–316 [PubMed: 22546688]
35. Shuhaibar LC, Egbert JR, Norris RP, Lampe PD, Nikolaev VO, Thunemann M, Wen L, Feil R, and Jaffe LA (2015) Intercellular signaling via cyclic GMP diffusion through gap junctions restarts meiosis in mouse ovarian follicles. Proc Natl Acad Sci U S A 112, 5527–5532 [PubMed: 25775542]
36. Jaffe LA, and Egbert JR (2017) Regulation of Mammalian Oocyte Meiosis by Intercellular Communication Within the Ovarian Follicle. Annu Rev Physiol 79, 237–260 [PubMed: 27860834]
37. Wagner BM, Robinson JW, Lin YW, Lee YC, Kaci N, Legeai-Mallet L, and Potter LR (2021) Prevention of guanylyl cyclase-B dephosphorylation rescues achondroplastic dwarfism. JCI Insight 6
38. Robinson JW, Blixt NC, Norton A, Mansky KC, Ye Z, Aparicio C, Wagner BM, Benton AM, Warren GL, Khosla S, Gaddy D, Suva LJ, and Potter LR (2020) Male mice with elevated C-type natriuretic peptide-dependent guanylyl cyclase-B activity have increased osteoblasts, bone mass and bone strength. Bone 135, 115320 [PubMed: 32179168]
39. John SW, Veress AT, Honrath U, Chong CK, Peng L, Smithies O, and Sonnenberg H (1996) Blood pressure and fluid-electrolyte balance in mice with reduced or absent ANP. Am J Physiol 271, R109–114 [PubMed: 8760210]
40. Oliver PM, John SW, Purdy KE, Kim R, Maeda N, Goy MF, and Smithies O (1998) Natriuretic peptide receptor 1 expression influences blood pressures of mice in a dose-dependent manner. Proc Natl Acad Sci U S A 95, 2547–2551 [PubMed: 9482923]
41. Suda M, Ogawa Y, Tanaka K, Tamura N, Yasoda A, Takigawa T, Uehira M, Nishimoto H, Itoh H, Saito Y, Shiota K, and Nakao K (1998) Skeletal overgrowth in transgenic mice that overexpress brain natriuretic peptide. Proceedings of the National Academy of Sciences of the United States of America 95, 2337–2342 [PubMed: 9482886]
42. Hori R, Inui K, Saito H, Matsukawa Y, Okumura K, Nakao K, Morii N, and Imura H (1985) Specific receptors for atrial natriuretic polypeptide on basolateral membranes isolated from rat renal cortex. Biochem Biophys Res Commun 129, 773–779 [PubMed: 2990466]
43. Tamura N, Ogawa Y, Chusho H, Nakamura K, Nakao K, Suda M, Kasahara M, Hashimoto R, Katsuura G, Mukoyama M, Itoh H, Saito Y, Tanaka I, Otani H, and Katsuki M (2000) Cardiac fibrosis in mice lacking brain natriuretic peptide. Proc Natl Acad Sci U S A 97, 4239–4244 [PubMed: 10737768]
44. Coué M, Badin PM, Vila IK, Laurens C, Louche K, Marquès MA, Bourlier V, Mouisel E, Tavernier G, Rustan AC, Galgani JE, Joanisse DR, Smith SR, Langin D, and Moro C (2015) Defective Natriuretic Peptide Receptor Signaling in Skeletal Muscle Links Obesity to Type 2 Diabetes. Diabetes 64, 4033–4045 [PubMed: 26253614]

45. Miyashita K, Itoh H, Tsujimoto H, Tamura N, Fukunaga Y, Sone M, Yamahara K, Taura D, Inuzuka M, Sonoyama T, and Nakao K (2009) Natriuretic peptides/cGMP/cGMP-dependent protein kinase cascades promote muscle mitochondrial biogenesis and prevent obesity. Diabetes 58, 2880–2892 [PubMed: 19690065]

46. Abbey SE, and Potter LR (2002) Vasopressin-dependent inhibition of the C-type natriuretic peptide receptor, NPR-B/GC-B, requires elevated intracellular calcium concentrations. The Journal of biological chemistry 277, 42423–42430 [PubMed: 12196532]

47. Dickey DM, Yoder AR, and Potter LR (2009) A familial mutation renders atrial natriuretic Peptide resistant to proteolytic degradation. The Journal of biological chemistry 284, 19196–19202 [PubMed: 19458086]

48. Edmund AB, Walseth TF, Levinson NM, and Potter LR (2019) The pseudokinase domains of guanylyl cyclase-A and -B allosterically increase the affinity of their catalytic domains for substrate. Sci Signal 12

49. Domino SE, Tubb DJ, and Garbers DL (1991) Assay of guanylyl cyclase catalytic activity. Methods Enzymol 195, 345–355 [PubMed: 1674565]

50. Asirvatham-Jeyaraj N, Gauthier MM, Banek CT, Ramesh A, Garver H, Fink GD, and Osborn JW (2021) Renal Denervation and Celiac Ganglionectomy Decrease Mean Arterial Pressure Similarly in Genetically Hypertensive Schlager (BPH/2J) Mice. Hypertension 77, 519–528 [PubMed: 33390041]

51. O'Connell TD, Swigart PM, Rodrigo MC, Ishizaka S, Joho S, Turnbull L, Tecott LH, Baker AJ, Foster E, Grossman W, and Simpson PC (2006) Alpha1-adrenergic receptors prevent a maladaptive cardiac response to pressure overload. J Clin Invest 116, 1005–1015 [PubMed: 16585965]

52. O'Connell TD, Ishizaka S, Nakamura A, Swigart PM, Rodrigo MC, Simpson GL, Cotecchia S, Rokosh DG, Grossman W, Foster E, and Simpson PC (2003) The alpha(1A/C)- and alpha(1B)-adrenergic receptors are required for physiological cardiac hypertrophy in the double-knockout mouse. J Clin Invest 111, 1783–1791 [PubMed: 12782680]

53. Keppler A, Gretz N, Schmidt R, Kloetzer H-M, Groene H-J, Lelongt B, Meyer M, Sadick M, and Pill J (2007) Plasma creatinine determination in mice and rats: An enzymatic method compares favorably with a high-performance liquid chromatography assay. Kidney International 71, 74–78 [PubMed: 17082757]

54. Marin-Grez M, Fleming JT, and Steinhausen M (1986) Atrial natriuretic peptide causes pre-glomerular vasodilatation and post-glomerular vasoconstriction in rat kidney. Nature 324, 473–476 [PubMed: 2946962]

55. Schewe J, Seidel E, Forslund S, Marko L, Peters J, Muller DN, Fahlke C, Stölting G, and Scholl U (2019) Elevated aldosterone and blood pressure in a mouse model of familial hyperaldosteronism with ClC-2 mutation. Nat Commun 10, 5155 [PubMed: 31727896]

56. Li Y, Kishimoto I, Saito Y, Harada M, Kuwahara K, Izumi T, Hamanaka I, Takahashi N, Kawakami R, Tanimoto K, Nakagawa Y, Nakanishi M, Adachi Y, Garbers DL, Fukamizu A, and Nakao K (2004) Androgen contributes to gender-related cardiac hypertrophy and fibrosis in mice lacking the gene encoding guanylyl cyclase-A. Endocrinology 145, 951–958 [PubMed: 14592959]

57. Pandey KN, Oliver PM, Maeda N, and Smithies O (1999) Hypertension associated with decreased testosterone levels in natriuretic peptide receptor-A gene-knockout and gene-duplicated mutant mouse models. Endocrinology 140, 5112–5119 [PubMed: 10537139]

58. Yan ZP, Li JT, Zeng N, and Ni GX (2020) Role of extracellular signal-regulated kinase 1/2 signaling underlying cardiac hypertrophy. Cardiol J

59. Ueyama T, Kawashima S, Sakoda T, Rikitake Y, Ishida T, Kawai M, Yamashita T, Ishido S, Hotta H, and Yokoyama M (2000) Requirement of activation of the extracellular signal-regulated kinase cascade in myocardial cell hypertrophy. J Mol Cell Cardiol 32, 947–960 [PubMed: 10888249]

60. Rose BA, Force T, and Wang Y (2010) Mitogen-activated protein kinase signaling in the heart: angels versus demons in a heart-breaking tale. Physiol Rev 90, 1507–1546 [PubMed: 20959622]

61. Hayashi D, Kudoh S, Shiojima I, Zou Y, Harada K, Shimoyama M, Imai Y, Monzen K, Yamazaki T, Yazaki Y, Nagai R, and Komuro I (2004) Atrial natriuretic peptide inhibits cardiomyocyte

hypertrophy through mitogen-activated protein kinase phosphatase-1. Biochem Biophys Res Commun 322, 310–319 [PubMed: 15313208]

62. Sugimoto T, Kikkawa R, Haneda M, and Shigeta Y (1993) Atrial natriuretic peptide inhibits endothelin-1-induced activation of mitogen-activated protein kinase in cultured rat mesangial cells. Biochem Biophys Res Commun 195, 72–78 [PubMed: 8395837]
63. Pandey KN, Nguyen HT, Li M, and Boyle JW (2000) Natriuretic peptide receptor-A negatively regulates mitogen-activated protein kinase and proliferation of mesangial cells: role of cGMP-dependent protein kinase. Biochem Biophys Res Commun 271, 374–379 [PubMed: 10799305]
64. Hodgson-Zingman DM, Karst ML, Zingman LV, Heublein DM, Darbar D, Herron KJ, Ballew JD, de Andrade M, Burnett JC Jr., and Olson TM (2008) Atrial natriuretic peptide frameshift mutation in familial atrial fibrillation. N Engl J Med 359, 158–165 [PubMed: 18614783]
65. Chen Y, Schaefer JJ, Iyer SR, Harders GE, Pan S, Sangaralingham SJ, Chen HH, Redfield MM, and Burnett JC (2020) Long-term blood pressure lowering and cGMP-activating actions of the novel ANP analog MANP. Am J Physiol Regul Integr Comp Physiol 318, R669–R676 [PubMed: 32022596]
66. Koller KJ, Lipari MT, and Goeddel DV (1993) Proper glycosylation and phosphorylation of the type A natriuretic peptide receptor are required for hormone-stimulated guanylyl cyclase activity. The Journal of biological chemistry 268, 5997–6003 [PubMed: 8095500]
67. Schröter J, Zahedi RP, Hartmann M, Gassner B, Gazinski A, Waschke J, Sickmann A, and Kuhn M (2010) Homologous desensitization of guanylyl cyclase A, the receptor for atrial natriuretic peptide, is associated with a complex phosphorylation pattern. FEBS J 277, 2440–2453 [PubMed: 20456499]
68. Nushiro N, Abe K, Seino M, Itoh S, and Yoshinaga K (1987) The effects of atrial natriuretic peptide on renal function and the renin-aldosterone system in anesthetized rabbits. Tohoku J Exp Med 152, 301–310 [PubMed: 2958960]
69. Vellaichamy E, Das S, Subramanian U, Maeda N, and Pandey KN (2014) Genetically altered mutant mouse models of guanylyl cyclase/natriuretic peptide receptor-A exhibit the cardiac expression of proinflammatory mediators in a gene-dose-dependent manner. Endocrinology 155, 1045–1056 [PubMed: 24424043]
70. Otani K, Tokudome T, Kamiya CA, Mao Y, Nishimura H, Hasegawa T, Arai Y, Kaneko M, Shioi G, Ishida J, Fukamizu A, Osaki T, Nagai-Okatani C, Minamino N, Ensho T, Hino J, Murata S, Takegami M, Nishimura K, Kishimoto I, Miyazato M, Harada-Shiba M, Yoshimatsu J, Nakao K, Ikeda T, and Kangawa K (2020) Deficiency of Cardiac Natriuretic Peptide Signaling Promotes Peripartum Cardiomyopathy-Like Remodeling in the Mouse Heart. Circulation 141, 571–588 [PubMed: 31665900]
71. Huang PL, Huang Z, Mashimo H, Bloch KD, Moskowitz MA, Bevan JA, and Fishman MC (1995) Hypertension in mice lacking the gene for endothelial nitric oxide synthase. Nature 377, 239–242 [PubMed: 7545787]
72. Tsai EJ, and Kass DA (2009) Cyclic GMP signaling in cardiovascular pathophysiology and therapeutics. Pharmacol Ther 122, 216–238 [PubMed: 19306895]
73. Lee DI, Zhu G, Sasaki T, Cho GS, Hamdani N, Holewinski R, Jo SH, Danner T, Zhang M, Rainer PP, Bedja D, Kirk JA, Ranek MJ, Dostmann WR, Kwon C, Margulies KB, Van Eyk JE, Paulus WJ, Takimoto E, and Kass DA (2015) Phosphodiesterase 9A controls nitric-oxide-independent cGMP and hypertrophic heart disease. Nature 519, 472–476 [PubMed: 25799991]
74. Yasoda A, Komatsu Y, Chusho H, Miyazawa T, Ozasa A, Miura M, Kurihara T, Rogi T, Tanaka S, Suda M, Tamura N, Ogawa Y, and Nakao K (2004) Overexpression of CNP in chondrocytes rescues achondroplasia through a MAPK-dependent pathway. Nat Med 10, 80–86 [PubMed: 14702637]
75. Suhasini M, Li H, Lohmann SM, Boss GR, and Pilz RB (1998) Cyclic-GMP-dependent protein kinase inhibits the Ras/Mitogen-activated protein kinase pathway. Mol Cell Biol 18, 6983–6994 [PubMed: 9819386]
76. Lukowski R, Rybalkin SD, Loga F, Leiss V, Beavo JA, and Hofmann F (2010) Cardiac hypertrophy is not amplified by deletion of cGMP-dependent protein kinase I in cardiomyocytes. Proc Natl Acad Sci U S A 107, 5646–5651 [PubMed: 20212138]

77. Patrucco E, Domes K, Sbroggió M, Blaich A, Schlossmann J, Desch M, Rybalkin SD, Beavo JA, Lukowski R, and Hofmann F (2014) Roles of cGMP-dependent protein kinase I (cGKI) and PDE5 in the regulation of Ang II-induced cardiac hypertrophy and fibrosis. Proc Natl Acad Sci U S A 111, 12925–12929 [PubMed: 25139994]

78. Hofmann F (2018) A concise discussion of the regulatory role of cGMP kinase I in cardiac physiology and pathology. Basic Res Cardiol 113, 31 [PubMed: 29934662]

79. Nakamura M, and Sadoshima J (2018) Mechanisms of physiological and pathological cardiac hypertrophy. Nat Rev Cardiol 15, 387–407 [PubMed: 29674714]

80. Purcell NH, Wilkins BJ, York A, Saba-El-Leil MK, Meloche S, Robbins J, and Molkentin JD (2007) Genetic inhibition of cardiac ERK1/2 promotes stress-induced apoptosis and heart failure but has no effect on hypertrophy in vivo. Proc Natl Acad Sci U S A 104, 14074–14079 [PubMed: 17709754]

81. Kehat I, and Molkentin JD (2010) Extracellular signal-regulated kinase 1/2 (ERK1/2) signaling in cardiac hypertrophy. Ann N Y Acad Sci 1188, 96–102 [PubMed: 20201891]

82. Bueno OF, De Windt LJ, Tymitz KM, Witt SA, Kimball TR, Klevitsky R, Hewett TE, Jones SP, Lefer DJ, Peng CF, Kitsis RN, and Molkentin JD (2000) The MEK1-ERK1/2 signaling pathway promotes compensated cardiac hypertrophy in transgenic mice. EMBO J 19, 6341–6350 [PubMed: 11101507]

83. Lips DJ, Bueno OF, Wilkins BJ, Purcell NH, Kaiser RA, Lorenz JN, Voisin L, Saba-El-Leil MK, Meloche S, Pouysségur J, Pagès G, De Windt LJ, Doevendans PA, and Molkentin JD (2004) MEK1-ERK2 signaling pathway protects myocardium from ischemic injury in vivo. Circulation 109, 1938–1941 [PubMed: 15096454]

84. Chen Y, Liu F, Chen BD, Li XM, Huang Y, Yu ZX, Gao XL, He CH, Yang YN, Ma YT, and Gao XM (2020) rAAV9-Mediated MEK1 Gene Expression Restores Post-conditioning Protection Against Ischemia Injury in Hypertrophic Myocardium. Cardiovasc Drugs Ther 34, 3–14 [PubMed: 32103377]

85. Silberbach M, Gorenc T, Hershberger RE, Stork PJ, Steyger PS, and Roberts CT (1999) Extracellular signal-regulated protein kinase activation is required for the anti-hypertrophic effect of atrial natriuretic factor in neonatal rat ventricular myocytes. J Biol Chem 274, 24858–24864 [PubMed: 10455158]

86. Babiker FA, De Windt LJ, van Eickels M, Thijssen V, Bronsaer RJ, Grohé C, van Bilsen M, and Doevendans PA (2004) 17beta-estradiol antagonizes cardiomyocyte hypertrophy by autocrine/paracrine stimulation of a guanylyl cyclase A receptor-cyclic guanosine monophosphate-dependent protein kinase pathway. Circulation 109, 269–276 [PubMed: 14718400]

87. van Eickels M, Grohé C, Cleutjens JP, Janssen BJ, Wellens HJ, and Doevendans PA (2001) 17beta-estradiol attenuates the development of pressure-overload hypertrophy. Circulation 104, 1419–1423 [PubMed: 11560859]

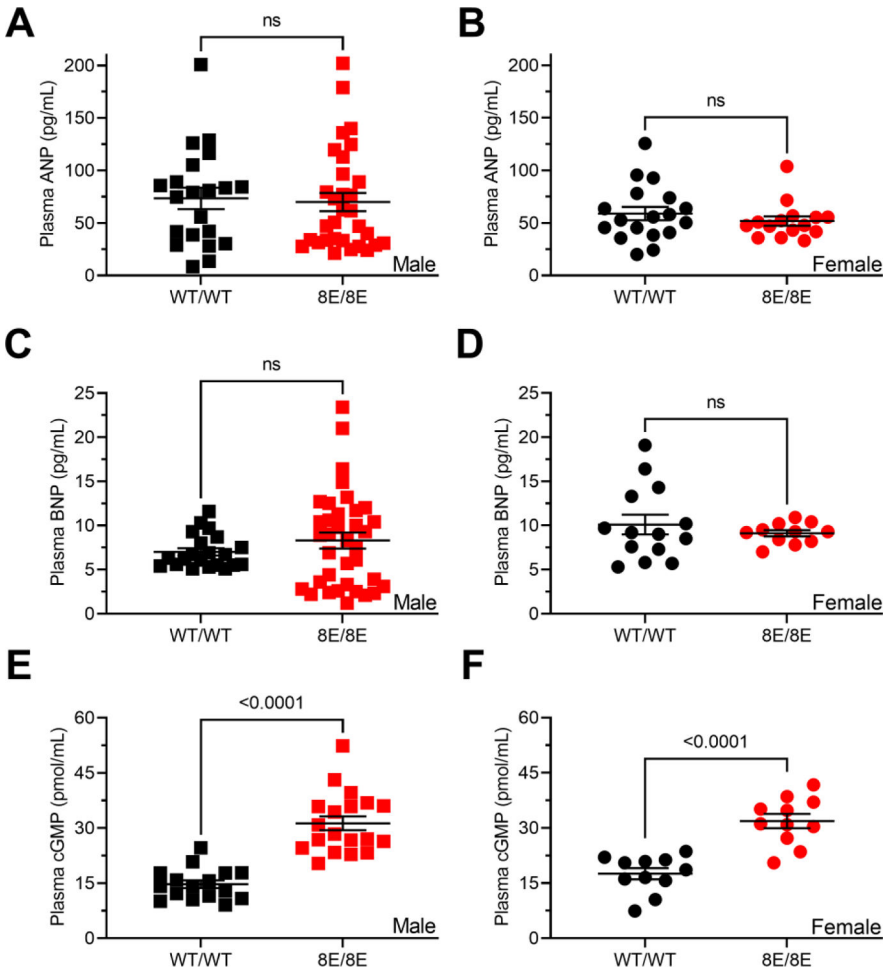


**Figure 1.**

GC-A$^{8E/8E}$ mice of both sexes have elevated plasma cGMP, but not NP concentrations. Plasma ANP, BNP and cGMP concentrations from GC-A$^{WT/WT}$ (black) or GC-A$^{8E/8E}$ (red) (A, C, E) male (squares) and (B, D, F) female (circles) mice. n = 11–36 mice per group. Statistical differences were determined using a two-tailed student's t-test with significant associated p values shown in each panel.

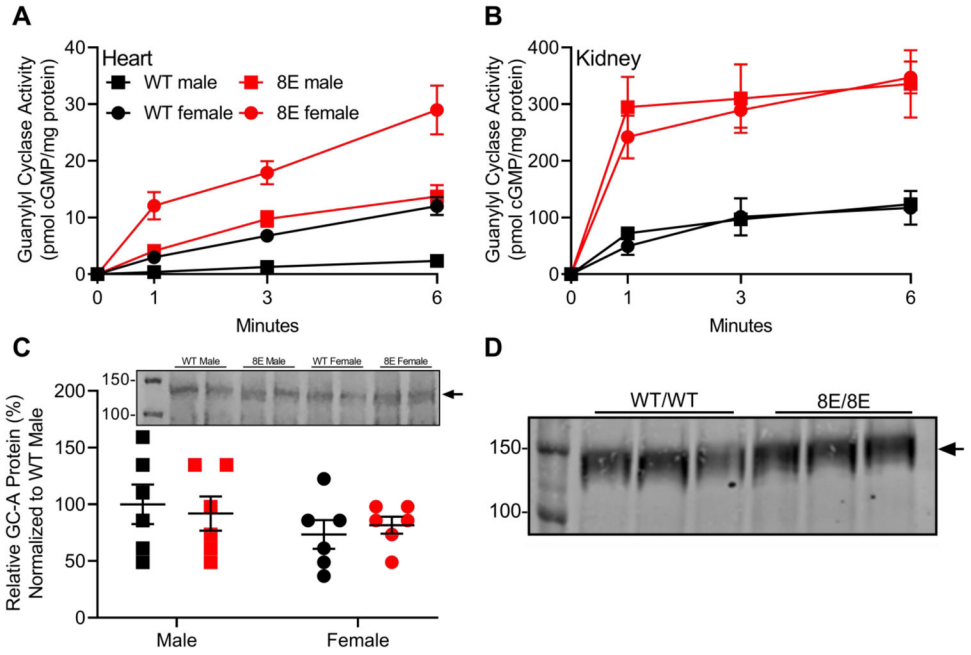


**Figure 2.**

GC-A$^{8E/8E}$ mice of both sexes have greater ANP-dependent guanylyl cyclase activity, but not GC-A protein levels, than GC-A$^{WT/WT}$ mice. Guanylyl cyclase activity determined in the presence of 1 μM ANP, 1 mM GTP, and 1 mM ATP in membranes from (A) cardiac ventricle or (B) whole kidney of male or female GC-A$^{WT/WT}$ and GC-A$^{8E/8E}$ mice. (C) Sequential immunoprecipitation-western blot analysis and quantitation of GC-A from individual GC-A$^{WT/WT}$ and GC-A$^{8E/8E}$ mouse hearts. (D) Sequential immunoprecipitation-western blot analysis of GC-A from male GC-A$^{WT/WT}$ and GC-A$^{8E/8E}$ mouse kidney membranes. Right arrows in panels C and D indicate GC-A. Numbers on the left side of panels C and D indicate 100 kDa and 150 kDa MW markers. Each lane in panel D represents the isolation of GC-A from one kidney from an individual mouse. For panels A-C, n = 6 per group. The symbols indicate the mean and the vertical bars within symbols indicate SEM. For panel C, no significant differences were observed between the groups.

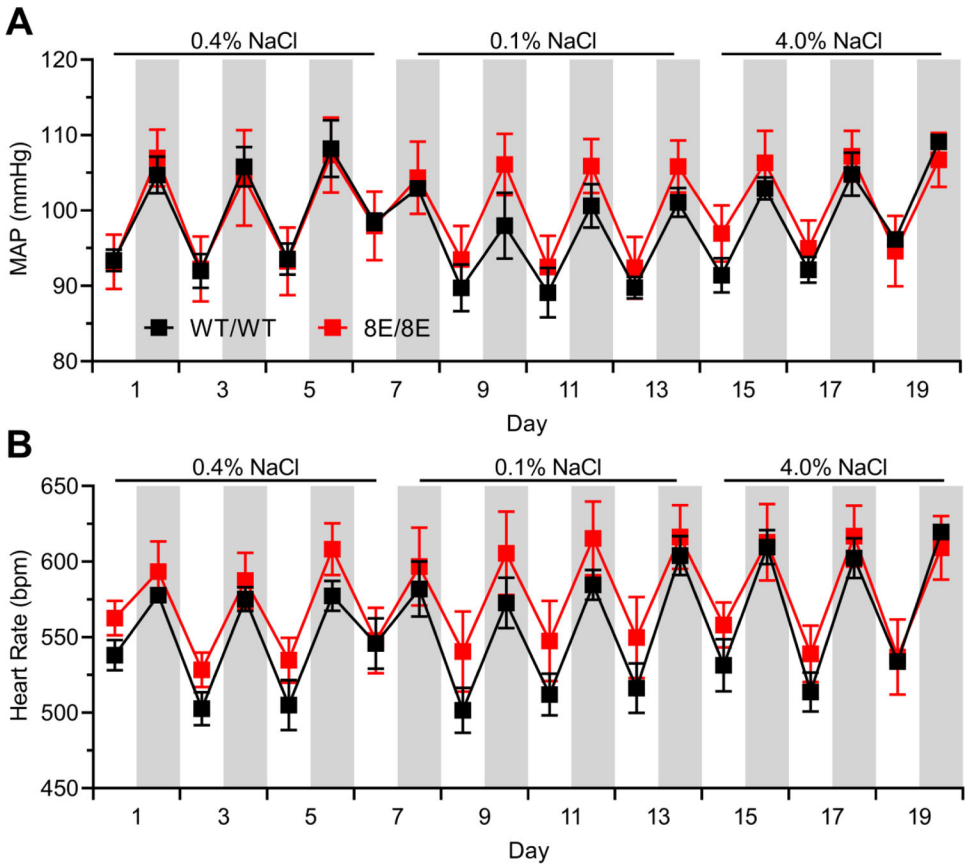


**Figure 3.**

Mean arterial pressure and heart rate do not differ between male GC-A$^{WT/WT}$ and GC-A$^{8E/8E}$ mice regardless of salt intake. (A) Mean arterial pressure (MAP) and (B) heart rate measured in beats per minute (bpm) for GC-A$^{WT/WT}$ and GC-A$^{8E/8E}$ in 16-week-old male mice fed the indicated dietary NaCl concentrations. n = 6 per group. White columns are “lights on” and gray columns are “lights off” measurements. The symbols indicate the mean and the vertical bars within symbols indicate SEM. Two-way repeated-measures ANOVA demonstrated no significant differences between GC-A$^{WT/WT}$ and GC-A$^{8E/8E}$ mice for either MAP or heart rate.

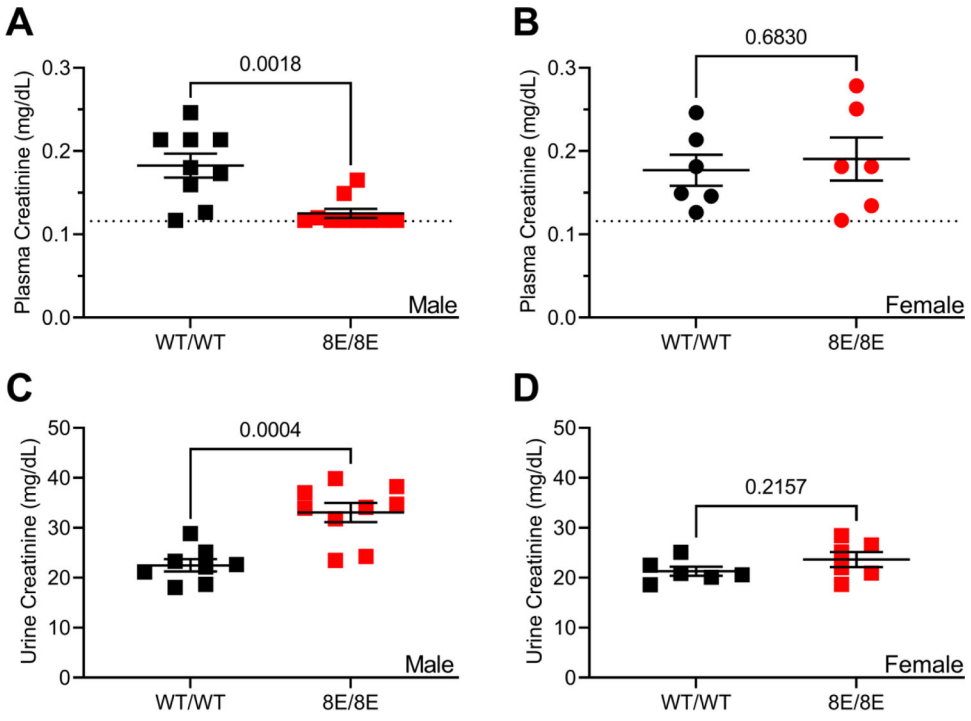


**Figure 4.**

GC-A$^{8E/8E}$ male mice have decreased plasma and increased urinary creatinine concentrations, respectively. Plasma and urine were collected from 12-week-old male and female mice. (A) Male and (B) female plasma creatinine concentrations. (C) Male and (D) female urine creatinine concentrations. Dotted line in panels A and B indicate the creatinine assay's limit of detection. n = 6–10 mice per group. Long horizontal bars indicate the mean and the shorter bars indicate SEM. Statistical differences were determined using a Mann-Whitney test for panels A and B. A two-tailed student's t-test was used to determine significance for panels C and D. Associated p values are shown in each panel for each test.

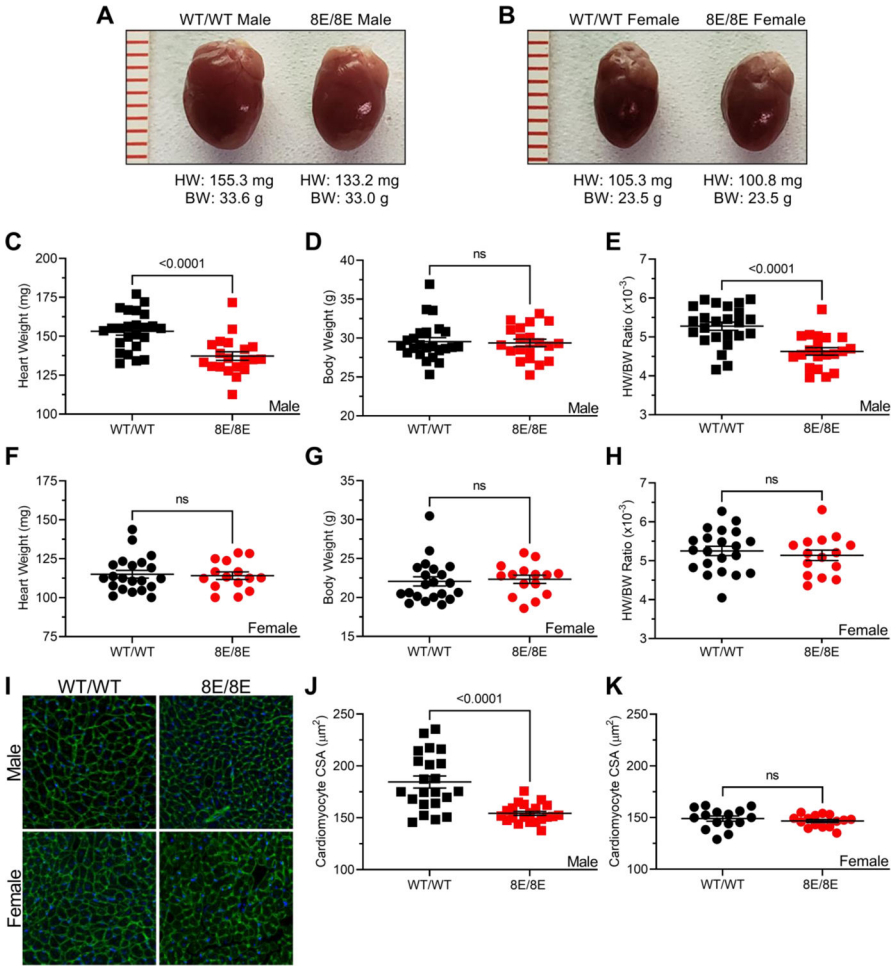


**Figure 5.**

Hearts from male GC-A$^{8E/8E}$ mice weigh less because they have smaller cardiomyocytes. Hearts from male and female GC-A$^{WT/WT}$ and GC-A$^{8E/8E}$ mice were collected for morphological analysis. Photos of (A) male and (B) female hearts from 12-week-old mice. Male (C) heart weight, (D) body weight, and (E) heart weight-to-body weight ratio (HW/BW). Female (F) heart weight, (G) body weight, and (H) HW/BW. Representative images of male and female cardiomyocyte (CM) cross sectional area (CSA) from ventricular tissue stained with WGA and DAPI (I). Quantitative results from (J) male and (K) female CM CSA analysis, which was performed with NIH ImageJ by measuring the CSA of 250 CM per heart and averaging the individual values for each heart. n = 15–24 mice per group. Long horizontal bars indicate the mean and vertical bars indicate SEM. Statistical differences were determined using a two-tailed student's t-test with associated p values shown in each panel.

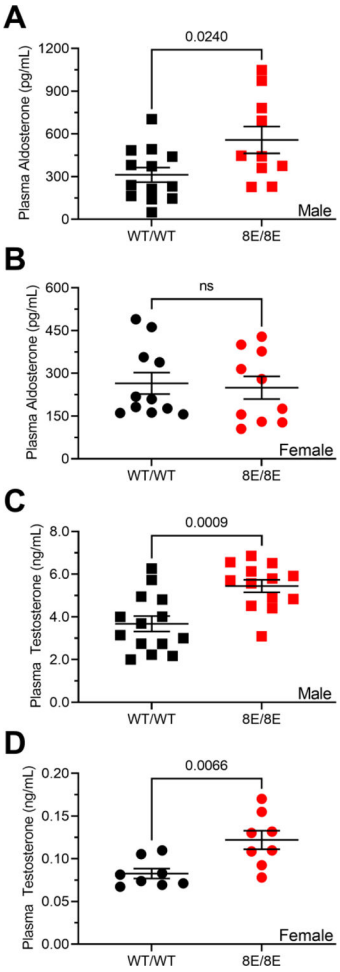


**Figure 6.**

Male GC-A$^{8E/8E}$ mice have elevated plasma aldosterone and testosterone concentrations. Plasma from male or female GC-A$^{WT/WT}$ and GC-A$^{8E/8E}$ mice was analyzed for aldosterone and testosterone concentrations by ELISAs. Male (A) and female (B) plasma aldosterone concentrations. Male (C) and female (D) plasma testosterone concentrations. n = 8–14 mice per group. Long horizontal bars indicate the mean and vertical bars indicate SEM. Statistical differences were determined using a two-tailed student's t-test with associated p values shown in each panel.

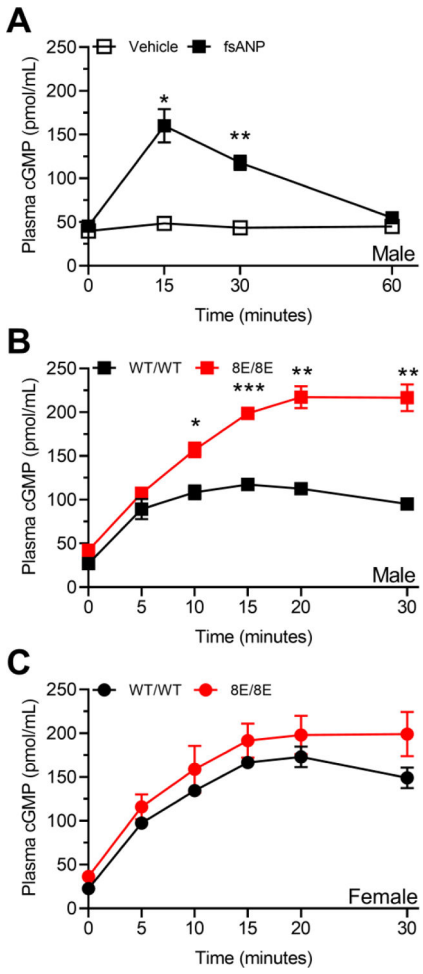


**Figure 7.**

fsANP injections result in a greater and more sustained elevation of plasma cGMP in male GC-A$^{8E/8E}$ compared to male GC-A$^{WT/WT}$ mice. (A) Injection of fsANP, but not saline vehicle, transiently increases plasma cGMP in male GC-A$^{WT/WT}$ mice. (B) Plasma cGMP concentrations in male GC-A$^{WT/WT}$ and GC-A$^{8E/8E}$ mice as a function of time after fsANP injection. (C) Plasma cGMP concentration in female GC-A$^{WT/WT}$ and GC-A$^{8E/8E}$ as a function of time after fsANP injection. The symbols represent the means and the vertical bars within the symbols represent the SEM. n = 3–5 mice per treatment. Statistically significant differences were determined by two-way-ANOVA with multiple comparisons where * = $p<0.05$, ** = $p<0.01$, and *** = $p<0.001$.

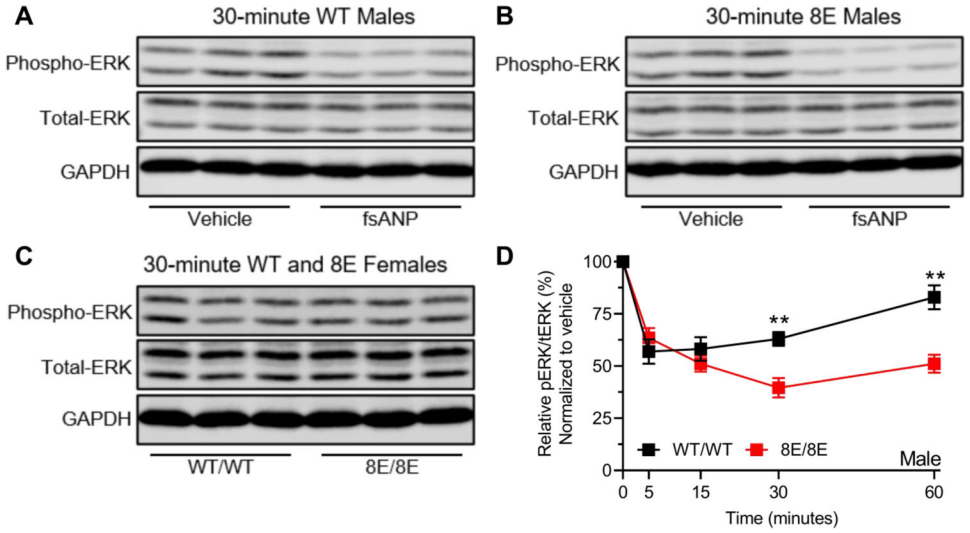


**Figure 8.**

fsANP injection suppresses ventricular ERK1/2 activity to a greater extent and for a longer period of time in male GC-A$^{8E/8E}$ compared to male GC-A$^{WT/WT}$ mice. Western blots of ventricular extracts probed for phospho-ERK1/2, total-ERK1/2, and GAPDH after injection with vehicle or fsANP in male GC-A$^{WT/WT}$ or GC-A$^{8E/8E}$ mice for (A and B) 30-minutes. (C) Western blot from female GC-A$^{WT/WT}$ and GC-A$^{8E/8E}$ mice 30 minutes after fsANP injection. (D) Relative ventricular ERK1/2 activities of male GC-A$^{WT/WT}$ and GC-A$^{8E/8E}$ mice normalized to vehicle control values as a function of time after fsANP injection. n = 4–7 mice per treatment. The symbols represent the means and the vertical bars within the symbols represent the SEM. Band intensities from left to right: (A) Phospho-ERK: 1.249, 1.586, 1.728, 0.750, 0.728, 0.969. Total-ERK: 1.859, 2.105, 2.008, 1.774, 1.603, 1.697. GAPDH: 5.663, 5.311, 4.923, 4.450, 4.777, 4.811. (B) Phospho-ERK: 1.244, 1.612,1.685, 0.493, 0.373, 0.482. Total-ERK: 1.822, 1.809, 1.904, 2.002, 1.658, 2.115. GAPDH: 4.893, 5.310, 5.661, 5.776, 5.273, 6.514. Statistically significant differences were determined by two-way-ANOVA with multiple comparisons where ** = $p<0.01$.

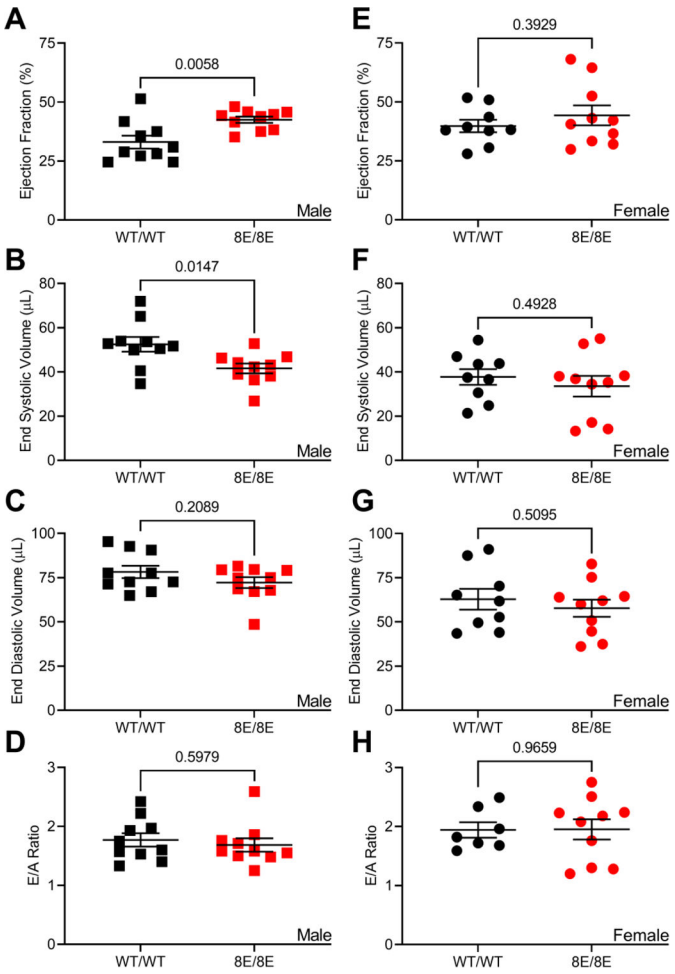


**Figure 9.**

Male, but not female, GC-A$^{8E/8E}$ hearts have improved systolic function. 12–13-week-old male (left panels) and female (right panels) GC-A$^{WT/WT}$ (black symbols) and GC-A$^{8E/8E}$ (red symbols) mice were assessed by echocardiography for (A, E) ejection fraction; (B, F) end systolic volume; (C, G) end diastolic volume; (D, H) E/A Ratio. n = 7–10 mice per group. Long horizontal bars indicate the mean and vertical bars indicate SEM. Statistical differences were determined using a two-tailed student's t-test with associated p values shown in each panel.